Molecular Cell
Article

# Methylation of a Histone Mimic within the Histone Methyltransferase G9a Regulates Protein Complex Assembly

Srihari C. Sampath,[1,*] Ivan Marazzi,[1] Kyoko L. Yap,[4] Srinath C. Sampath,[3] Andrew N. Krutchinsky,[2] Ingrid Mecklenbräuker,[1] Agnes Viale,[5] Eugene Rudensky,[1] Ming-Ming Zhou,[4] Brian T. Chait,[2] and Alexander Tarakhovsky[1,*]
[1] Laboratory of Lymphocyte Signaling
[2] Laboratory of Mass Spectrometry and Gaseous Ion Chemistry
[3] The Rockefeller University, New York, NY 10021, USA
[4] Department of Molecular Physiology and Biophysics, Mount Sinai School of Medicine, New York, NY 10029, USA
[5] Department of Molecular Biology/Genomics Core Laboratory, Memorial Sloan-Kettering Cancer Center, New York, NY 10021, USA
*Correspondence: sampasc@mail.rockefeller.edu (S.C.S.), tarakho@mail.rockefeller.edu (A.T.)
DOI 10.1016/j.molcel.2007.06.026

## SUMMARY

**Epigenetic gene silencing in eukaryotes is regulated in part by lysine methylation of the core histone proteins. While histone lysine methylation is known to control gene expression through the recruitment of modification-specific effector proteins, it remains unknown whether nonhistone chromatin proteins are targets for similar modification-recognition systems. Here we show that the histone H3 methyltransferase G9a contains a conserved methylation motif with marked sequence similarity to H3 itself. As with methylation of H3 lysine 9, autocatalytic G9a methylation is necessary and sufficient to mediate in vivo interaction with the epigenetic regulator heterochromatin protein 1 (HP1), and this methyl-dependent interaction can be reversed by adjacent G9a phosphorylation. NMR analysis indicates that the HP1 chromodomain recognizes methyl-G9a through a binding mode similar to that used in recognition of methyl-H3K9, demonstrating that the chromodomain functions as a generalized methyl-lysine binding module. These data reveal histone-like modification cassettes—or "histone mimics"—as a distinct class of nonhistone methylation targets and directly extend the principles of the histone code to the regulation of nonhistone proteins.**

## INTRODUCTION

Covalent modification of histones by methylation, phosphorylation, acetylation, and ubiquitination can modulate gene expression both directly, through effects on chromatin packaging, and indirectly, via recruitment of effector proteins (Strahl and Allis, 2000). Among the various histone modifications, lysine methylation stands out due to its multivalency, relative stability, and potential for functional crosstalk with other protein modifications (Byvoet et al., 1972; Fischle et al., 2003a). Methylation of histone 3 at lysine 9 (H3K9) has in particular served as the prototype for regulation of histone function by lysine methylation. Di- or trimethylation of H3K9 creates a binding site for chromodomain (CD)-containing proteins of the heterochromatin protein 1 (HP1) family (Bannister et al., 2001; Lachner et al., 2001), which is speculated to lead to gene repression via changes in higher-order chromatin structure. Methylation-dependent HP1 recruitment can be antagonized by adjacent H3 serine 10 phosphorylation, lending credence to the hypothesis that histones are subject to a system of combinatorially acting posttranslational modifications, sometimes referred to as the "histone code" (Fischle et al., 2005; Hirota et al., 2005; Strahl and Allis, 2000).

Although much attention has been directed toward elucidating the principles underlying histone modification, it has been known for many years that nonhistone proteins are also targets for many of the same categories of modification, including methylation (Paik and Kim, 1971). Recent work has expanded the list of lysine-methylated nonhistone proteins to include the tumor suppressor p53, the mitotic regulator Dam1, and the TFIID component TAF10 (Chuikov et al., 2004; Huang et al., 2006; Kouskouti et al., 2004; Zhang et al., 2005). In contrast, little progress has been made in identifying nonhistone correlates of the modification-recognition systems which characterize histone lysine methylation (e.g., meH3K4/K9/K27/K36/K79 and meH4K20; for review, see Kouzarides, 2007). For this reason, it has been impossible to determine whether the principles of regulation encompassed by the histone code hypothesis represent a peculiarity of histone biology

or whether they in fact represent a particular instance of a potentially more universal "protein code" (Margueron et al., 2005).

Here we demonstrate that the essential H3K9 methyltransferase G9a is lysine methylated on multiple H3K9-like sites in vivo. We further show that methylation of one of these sites recapitulates many aspects of H3K9 regulation, including methylation to multiple valencies, structural recognition and binding by modification-specific effector proteins, and reversibility of effector binding by concomitant phosphorylation. These findings reveal that both the modification and recognition systems governing the methyl-H3K9 epigenetic mark are conserved in a nonhistone protein, constituting one instance of a phenomenon that we refer to as "histone mimicry." On the basis of these data, we suggest that the core tenets of the histone code hypothesis are of much broader relevance than previously appreciated and are in fact applicable to nonhistone proteins as well.

## RESULTS

### The Histone Methyltransferase G9a Is Lysine Methylated In Vivo

G9a is a member of the Suvar(3–9) family of SET domain HMTases, all members of which methylate lysine 9 of H3 (Dillon et al., 2005; Rea et al., 2000). In addition to G9a, this family also includes a G9a-like protein known as GLP or EuHMTase-1 (Ogawa et al., 2002). Alignment of the amino termini of murine G9a and GLP identified an identical stretch of eight amino acids that strongly resembled the H3K9 methylation site targeted by both G9a and GLP (Figure 1A). This sequence was conserved in the G9a homolog from *Xenopus*, and the core motif was also found in *Drosophila* G9a (Figure 1A).

We hypothesized that the similar sequence context of G9a K165 and H3K9 could allow G9a K165 lysine methylation in vivo. Indeed, we found that a "multimethyl" lysine-specific antibody originally raised against a branched-peptide H3K9 me2 antigen (α4xH3K9me2; Perez-Burgos et al., 2004) recognized both a chemically methylated G9a K165 peptide (Figure 1B) as well as endogenous G9a immunoprecipitated using an affinity-purified N-terminal G9a antibody (αG9a-N; Figure 1C and see Figure S1 in the Supplemental Data available with this article online). Furthermore, an antibody raised specifically against dimethylated G9a K165 (Figure 1D) recognized both full-length endogenous G9a and an alternatively transcribed G9a isoform (Figure 1E, asterisk; Tachibana et al., 2002), demonstrating that G9a is dimethylated on K165 in vivo. In addition to G9a, the αK165 me2 antibody also recognized an ~200 kD protein (Figure 1E, arrowhead). Analysis of this protein by mass spectrometry (MS) identified it as the human homolog of mAM, a critical component of the ESET H3K9 methyltransferase complex (Wang et al., 2003; Figure S2A, see the Discussion).

Digestion of immunoprecipitated G9a (Figure S3A, asterisk) with trypsin, followed by MS, revealed that dimethylated K165 represents just one of several methylated G9a species in vivo (Figure S3B). One MS peak not corresponding to predicted G9a peptides represented a G9a fragment carrying trimethyl K165, as shown by the characteristic loss of 59 Da upon fragmentation (Figure 2A, left). Trimethylation on K165 was further confirmed by MS/MS/MS analysis of the modified peptide (Figure S4A). In addition to K165, we also identified two MS peaks representing a G9a peptide bearing di- and trimethylation of an additional lysine, K94 (Figure 2A, right, and Figure S4B). Strikingly, as with G9a K165, G9a K94 exists in a sequence context resembling H3K9 (Figure 2B). Although both G9a K165 and K94 are sites of endogenous di- and trimethylation, only the K165 site is recognized by the α4xH3K9me2 and αK165me2 antibodies (Figure 2C).

### G9a Is a Self-Methylating Lysine Methyltransferase

The sequence similarity between H3K9 and G9a K165 raised the possibility of G9a self-methylation. Indeed, we found that G9a was capable of methylating an unmodified G9a K165 peptide in vitro (Figure S5), while the related H3K9 methyltransferase Suv39H1 could not (data not shown). To test whether G9a catalyzes its own methylation, we created G9a-deficient cells reconstituted with either catalytically active or inactive G9a, as only the catalytically active protein would be expected to undergo K165 methylation upon expression in cells otherwise lacking G9a.

G9a-deficient cells were created by conditional inactivation of murine *G9a* using Cre-*lox*P technology. Gene targeting was used to produce embryonic stem (ES) cells and mice bearing a *G9a* allele with a portion of the SET domain flanked by *lox*P sites ($G9a^{fl/fl}$; Figure 3A, left, and Figure S6A). G9a-deficient cells ($G9a^{\Delta/\Delta}$) were derived from $G9a^{fl/fl}$ primary mouse embryonic fibroblasts (MEFs) and were subsequently reconstituted with retroviruses encoding either empty vector ($G9a^{\Delta}$), FLAG-G9a ($G9a^{WT}$), FLAG-G9a K165A ($G9a^{K165A}$), or FLAG-G9a carrying an inactivating point mutation in the catalytic SET domain ($G9a^{H1093K}$; all cell lines are hereafter referred to as "reconstituted MEFs," see Figure 3A, right, for summary). PCR genotyping excluded the presence of residual $G9a^{fl/fl}$ cells (Figure S6B).

As expected, both $G9a^{\Delta}$ cells and those expressing catalytically inactive G9a ($G9a^{H1093K}$) showed a dramatic reduction in the overall level of H3K9 dimethylation (Figure 3B). Although both $G9a^{WT}$ and $G9a^{H1093K}$ were expressed at equal levels (Figure 3B), only the wild-type, but not the catalytically inactive G9a, was endogenously methylated as determined by western blot using the α4xH3K9 me2 antibody (Figure 3C). We conclude that G9a activity is required for G9a's own methylation on K165. Preliminary data from mixing experiments using catalytically active and inactive G9a indicate that this reaction occurs predominantly in *cis* (data not shown).

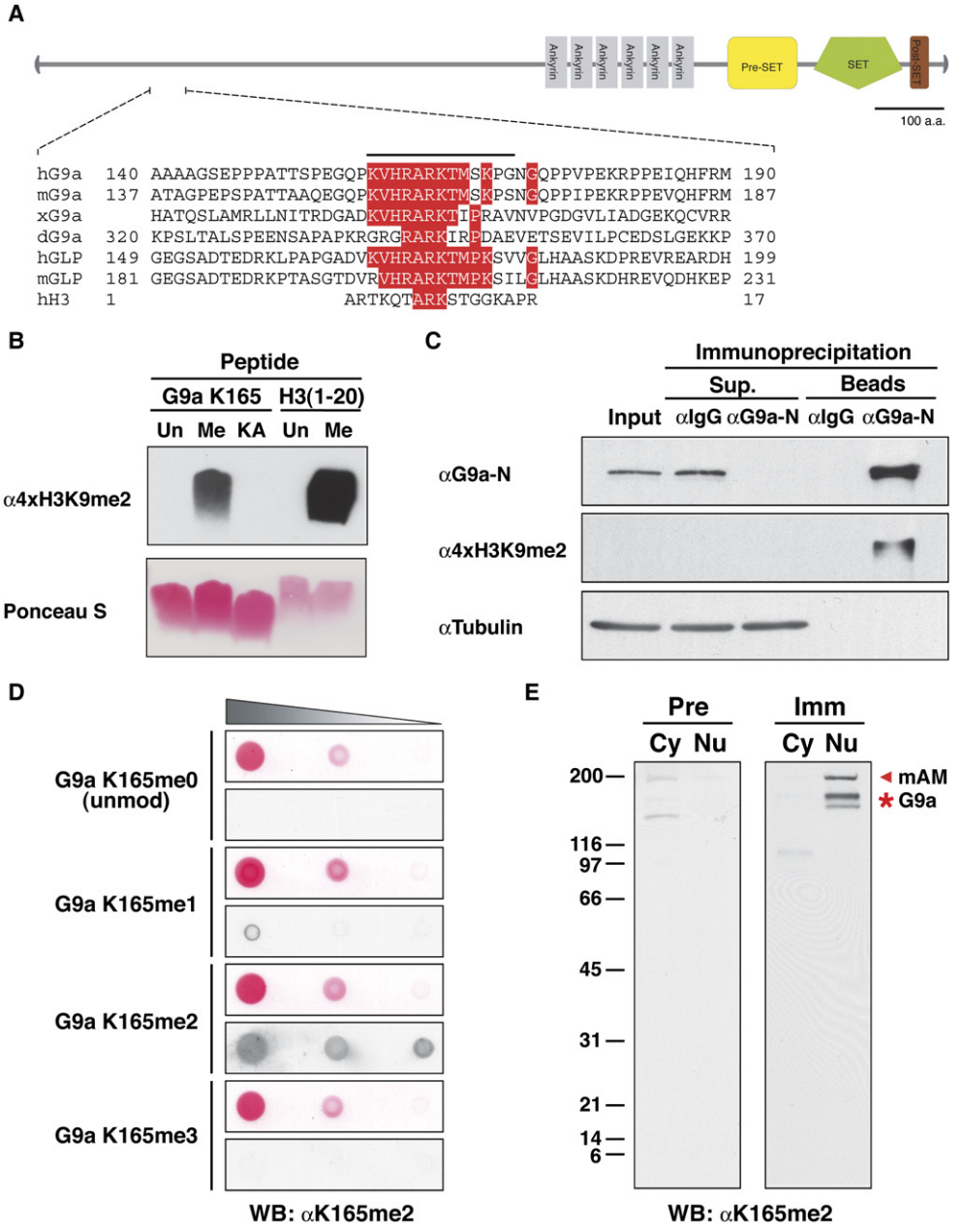


**Figure 1. The Histone Methyltransferase G9a Is Lysine Methylated In Vivo**

(A) An H3K9-like sequence is located in the noncatalytic N terminus of the G9a protein. (Top) Schematic representation of human G9a. (Bottom) Partial protein sequence alignment of G9a and GLP homologs from *Homo sapiens* (h), *Mus musculus* (m), *Xenopus laevis* (x), and *Drosophila melanogaster* (d), together with a portion of the human H3 amino-terminal tail. Residues identical in at least four of six sequences are highlighted in red, and the region used in G9a K165 peptides is indicated by a solid line. Residue numbers are indicated where known.

(B) Western blot analysis of G9a K165 and H3(1–20) peptides using a multimethyl α4xH3K9me2 antibody. Loading was monitored by Ponceau S staining, which preferentially stains the G9a peptide due to sequence effects (data not shown; Sarma et al. [2004]). Un, unmodified peptide; Me, peptide dimethylated at K165 (G9a) or K9 (H3); KA, G9a K165A mutant peptide.

(C) Endogenous G9a was immunoprecipitated from 293T cells using either control nonimmune antibody (αIgG) or an antibody raised against the G9a N terminus (αG9a-N; see Figure S1), followed by western blot using the antibodies indicated. α-tubulin blot was used to control for protein loading.

(D) The specificity of antibodies raised against dimethyl G9a K165 peptide (αK165me2) was assessed by dot blot analysis of 3-fold dilutions of the indicated peptides. Ponceau S staining control is shown above the corresponding dot blots.

(E) Western blot analysis of 293T cell cytosolic (Cy) and nuclear (Nu) extracts using either αK165me2 preimmune (left) or immune (right) serum. The molecular weight of endogenous hG9a is indicated with an asterisk, and the band corresponding to endogenous human mAM (hAM) is indicated with an arrowhead (see Figure S2 and the Discussion).

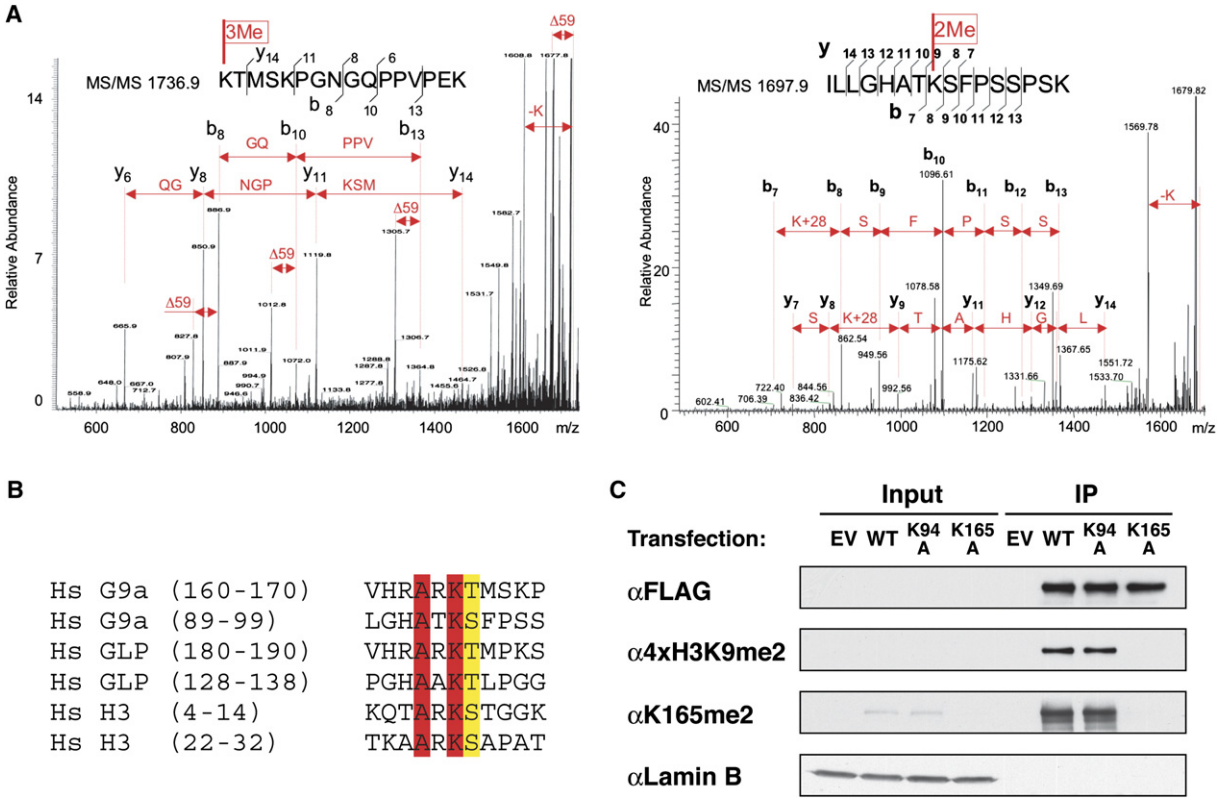


**Figure 2. G9a Is Methylated In Vivo on Multiple H3K9-like Sites**

(A) FLAG-G9a was purified from transiently transfected 293T cells, digested with trypsin, and analyzed by MS (see Figure S3). Ion peaks not assigned to tryptic G9a fragments were further analyzed by MS/MS. (Left) MALDI MS/MS spectrum of the tryptic peptide at m/z 1736.9 (KTMSKPGNGQPPVPEK), demonstrating the loss of 59 Da characteristic of trimethylation (Zhang et al., 2004). (Right) MS/MS spectrum of the peptides at m/z 1697.9 (ILLGHATKSFPSSPSK), representing dimethylation on K94.

(B) Sequence alignment of the region surrounding the human G9a K165 and K94 methylation sites, the corresponding sites in human GLP, and the sequence surrounding human H3K9 and H3K27. Residues identical in all sequences are shown in red and aligned putative phosphoacceptor sites in yellow.

(C) Wild-type FLAG-G9a or the indicated G9a mutants were expressed in 293T cells and immunoprecipitated, and G9a methylation was examined by western blot using the α4xH3K9me2 and αK165me2 antibodies. α-FLAG and α-lamin B blots were used to control for protein loading; input signal is visible in the α-FLAG blot on longer exposure (data not shown). EV, empty vector; WT, wild-type FLAG-G9a; K94A, FLAG-G9a K94A mutant; K165A, FLAG-G9a K165A mutant.

## G9a K165 Methylation Creates a Binding Site for HP1

G9a was previously shown to interact with HP1 and was found to exist in an in vivo complex containing the euchromatic HP1 isoform HP1γ (Ogawa et al., 2002; Roopra et al., 2004). Given the ability of HP1 to interact with methylated H3K9, we tested whether a similar mechanism might underlie the G9a-HP1 interaction. Incubation of immobilized unmodified, methylated, or K165A peptides with in vitro-translated HP1 isoforms demonstrated a specific role for G9a K165 methylation in promoting interaction with HP1 (Figure 4A). The K165 me2 peptide likewise interacted strongly with endogenous HP1γ and HP1α, whereas unmodified K165 peptide interacted only weakly (Figure 4B). The weak interaction observed with the unmodified peptide likely represents de novo methylation of K165, as it was completely blocked by mutation of K165 to alanine (Figure 4B). These results demonstrate that G9a-HP1 interaction can be mediated in a methylation-dependent manner by a minimal region encompassing the K165 methylation site.

To test whether K165 methylation is required for G9a-HP1 interaction in vivo, wild-type G9a or the G9a K165A mutant was expressed in 293T cells and assayed for their ability to associate with endogenous HP1. Immunoprecipitation of wild-type G9a led to coprecipitation of endogenous HP1γ, but this interaction was completely abolished by the G9a K165A mutation (Figure 4C). The effect of the K165A mutation on G9a-HP1γ interaction was specific, as the previously reported interaction between G9a and GLP was not affected by this mutation (data not shown). G9a K165 methylation is therefore both necessary and sufficient to mediate in vivo interaction between G9a and HP1.

The finding that HP1 specifically interacts with methylated G9a K165 raised the possibility that other proteins

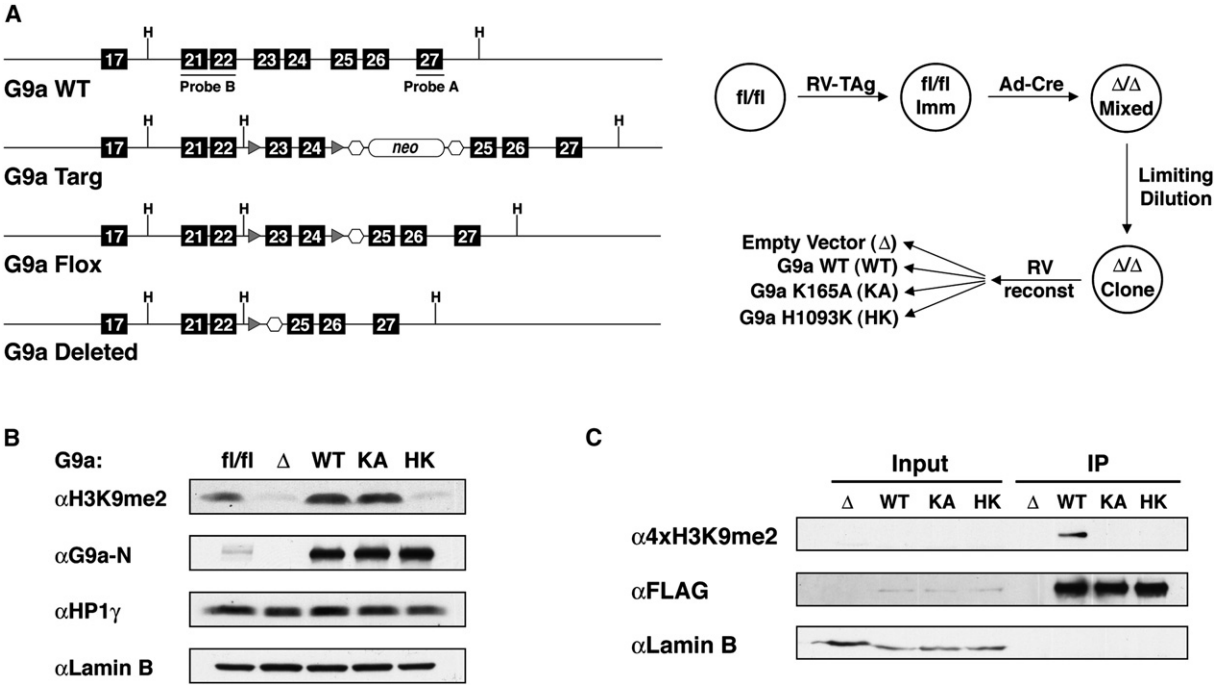


**Figure 3. Automethylation of G9a on K165 In Vivo**

(A) (Left) *G9a* conditional mutagenesis strategy. Exons 23 and 24 of the murine *G9a* locus were flanked by *lox*P sites (floxed), causing out-of-frame splicing and nonsense-mediated decay of the mutant transcript after Cre-mediated recombination (data not shown). Numbered box, exon; triangle, *lox*P site; hexagon, FRT site; *neo*, neomycin (G418) resistance cassette; H, HindIII restriction site. (Right) Strategy for production and reconstitution of G9a-deficient MEFs. G9a-deleted cells were reconstituted with either empty vector (Δ), wild-type FLAG-G9a (WT), FLAG-G9a K165A (KA), or FLAG-G9a H1093K catalytic mutant (HK). RV-TAg, retroviral SV40 large-T antigen; Imm, immortalized; Ad-Cre, adenoviral Cre.

(B) Nuclear lysates from $G9a^{fl/fl}$ (fl/fl) or reconstituted MEFs were analyzed by western blot using the indicated antibodies. α-lamin B blot was used to control for protein loading.

(C) Analysis of G9a automethylation. FLAG-G9a immunoprecipitated from the reconstituted MEFs described was analyzed by western blot using the α4xH3K9me2 antibody. Protein expression and loading were monitored by α-FLAG and α-lamin B blots, respectively.

might also bind to K165. Indeed, we found that immunoprecipitation of G9a led to copurification of CDYL (chromodomain Y-like; Figure S3A, arrowhead), a known transcriptional repressor containing an N-terminal chromodomain and a C-terminal coenzyme A-binding domain of unknown function (Caron et al., 2003). Consistent with its putative function as a transcriptional repressor, CDYL was previously copurified in an in vivo complex containing G9a, GLP, the transcriptional corepressor CtBP, and the histone lysine demethylase LSD1 (Shi et al., 2003).

By analogy to the G9a-HP1 interaction, we tested whether G9a K165 was necessary for G9a-CDYL interaction. Whereas wild-type G9a could coimmunoprecipitate endogenous CDYL from nuclear extracts, this interaction was completely lost in the G9a K165A mutant (Figure 4D), demonstrating that K165 serves as a binding site for both HP1 and CDYL. We therefore examined whether, as with HP1, K165 methylation mediates interaction with CDYL. Unlike HP1, the G9a-CDYL interaction could not be recapitulated in vitro using either unmodified, K165me, or K165meT166ph peptides (data not shown). Considering that CDYL exhibits HAT activity in vitro (Lahn et al., 2002) and has been suggested to acetylate nonhistone proteins (Caron et al., 2003), it is possible that CDYL binding is induced by alternative K165 modifications (e.g., phosphoacetylation or combinatorial lysine methylation), as was shown for the chromodomain-containing DNA methyltransferase CMT3 (Lindroth et al., 2004).

Taken together, these data demonstrate that G9a K165 is an in vivo binding site for multiple chromodomain-containing effector proteins. As recognition of methyl-G9a by HP1 to our knowledge represents the first nonhistone protein target for chromodomain binding, these results furthermore identify the chromodomain as a generalized methyl-lysine binding module.

## Structural Recognition of Methylated G9a

To address the structural basis for HP1 recognition of both methylated H3K9 and methylated G9a K165, we used nuclear magnetic resonance (NMR) spectroscopy to study both sets of interactions. In the absence of lysine-methylated G9a K165 peptide, the backbone amide resonances of $^{15}$N-labeled HP1γ chromodomain (CD) were well-dispersed in the 2D [$^{15}$N,$^{1}$H]-HSQC (heteronuclear single quantum coherence) spectrum, indicating a folded protein (Figure 5A). Upon addition of trimethylated G9a

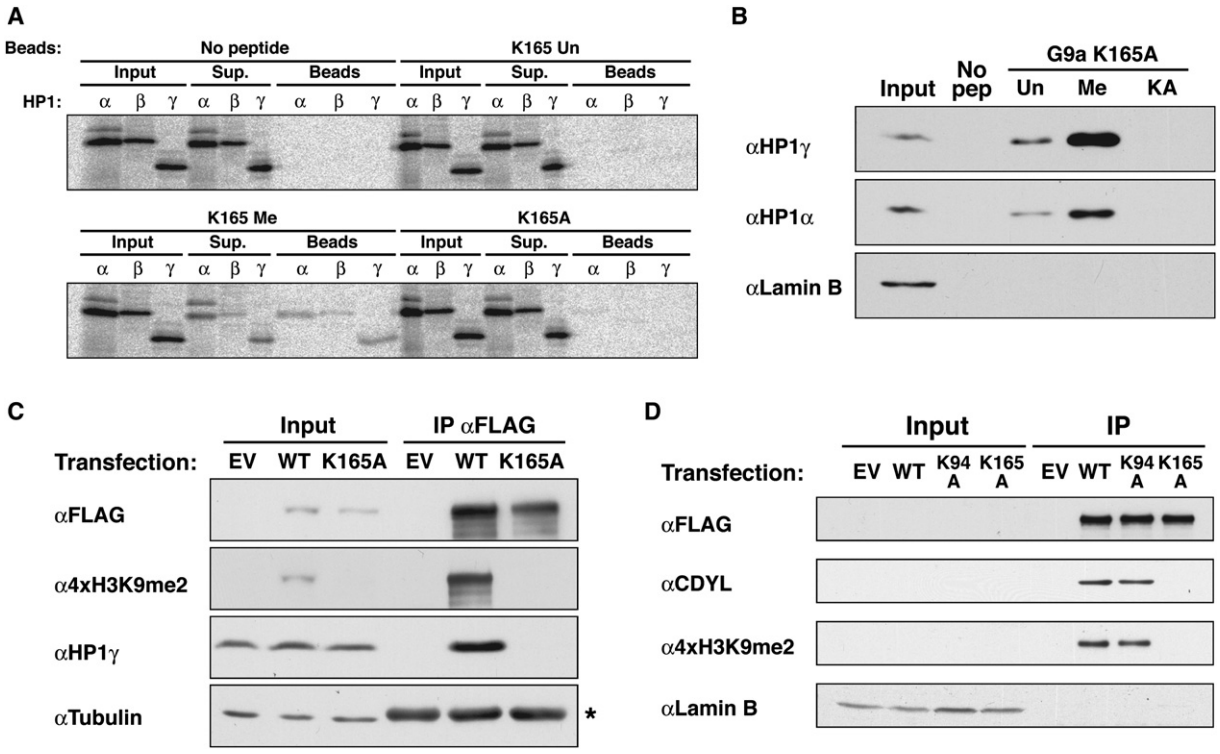


**Figure 4. G9a K165 Methylation Is Necessary and Sufficient for Interaction with HP1**

(A) Interaction between HP1 and G9a peptides in vitro. Beads coupled with either no peptide or the indicated G9a K165 peptides were incubated with in vitro-translated, $^{35}$S-radiolabeled HP1 isoforms. After extensive washing, the recovered protein was examined by SDS-PAGE and autoradiography. HP1 isoforms are codepleted with the methylated G9a K165 peptide (compare protein levels in input versus supernatant samples), but not with the unmodified or K165A mutant peptides. K165 Un, unmodified peptide; K165 Me, dimethylated peptide; K165A, mutant peptide.

(B) G9a interaction with HP1γ requires K165. G9a peptides covalently coupled to beads were incubated with 293T cell nuclear extract and washed extensively, and the recovered protein was analyzed by western blot analysis using the indicated antibodies. Beads were coupled with either no peptide (No pep), or G9a K165 unmodified (Un), dimethylated (Me), or K165A mutant (KA) peptides.

(C) Wild-type FLAG-G9a or FLAG-G9a K165A mutant was expressed in 293T cells and immunoprecipitated, and western blot was performed using the indicated antibodies. Asterisk indicates immunoglobulin heavy-chain crossreaction with the α-tubulin antibody. EV, empty vector control transfection.

(D) 293T cells were transfected with plasmids encoding either empty vector (EV), wild-type FLAG-G9a (WT), or the indicated G9a point mutants, and the expressed protein immunoprecipitated and analyzed by western blot using the antibodies listed. Input protein is visible in the α-FLAG blot on longer exposure (data not shown).

K165 peptide, several HP1 resonances were perturbed as a function of ligand concentration; migration of these peaks saturated at equimolar peptide and protein concentrations, confirming direct interaction between HP1γ CD and K165me3 (Figure 5A and Figure S7A, right).

A number of protein resonances that disappeared upon peptide addition (due to line broadening) correspond to residues that are in intermediate chemical exchange on the NMR timescale, suggesting a low micromolar affinity. Interestingly, addition of a dimethylated G9a K165 peptide to HP1γ CD resulted in chemical shift changes similar to those imposed by the K165me3 peptide; however, many of these shifts did not saturate at the concentrations tested, implying a weaker interaction (Figure 5A). Titration of a G9a peptide di- or trimethylated at K94 into the HP1γ CD sample induced no change in the HSQC spectra other than a few chemical shifts that did not saturate at the maximum concentration tested (0.5 mM) but underwent a linearly dependent change in response to peptide concentration, indicating very weak or nonspecific binding to methylated K94 (Figure S7B).

Consistent with previous reports, NMR analysis also demonstrated specific binding of the HP1γ CD to a H3(1–20) peptide trimethylated at K9 (Figure 5B). Importantly, the 2D [$^{15}$N,$^{1}$H]-HSQC HP1γ CD spectra exhibited chemical shift perturbations upon addition of H3K9me3 that were similar to those caused by binding to G9a K165me3 (Figure 5B), indicating that a set of the same chromodomain residues are involved in this interaction. Furthermore, the chemical shifts saturate at similar concentrations, implying comparable affinities of HP1γ for G9a K165 and for H3K9.

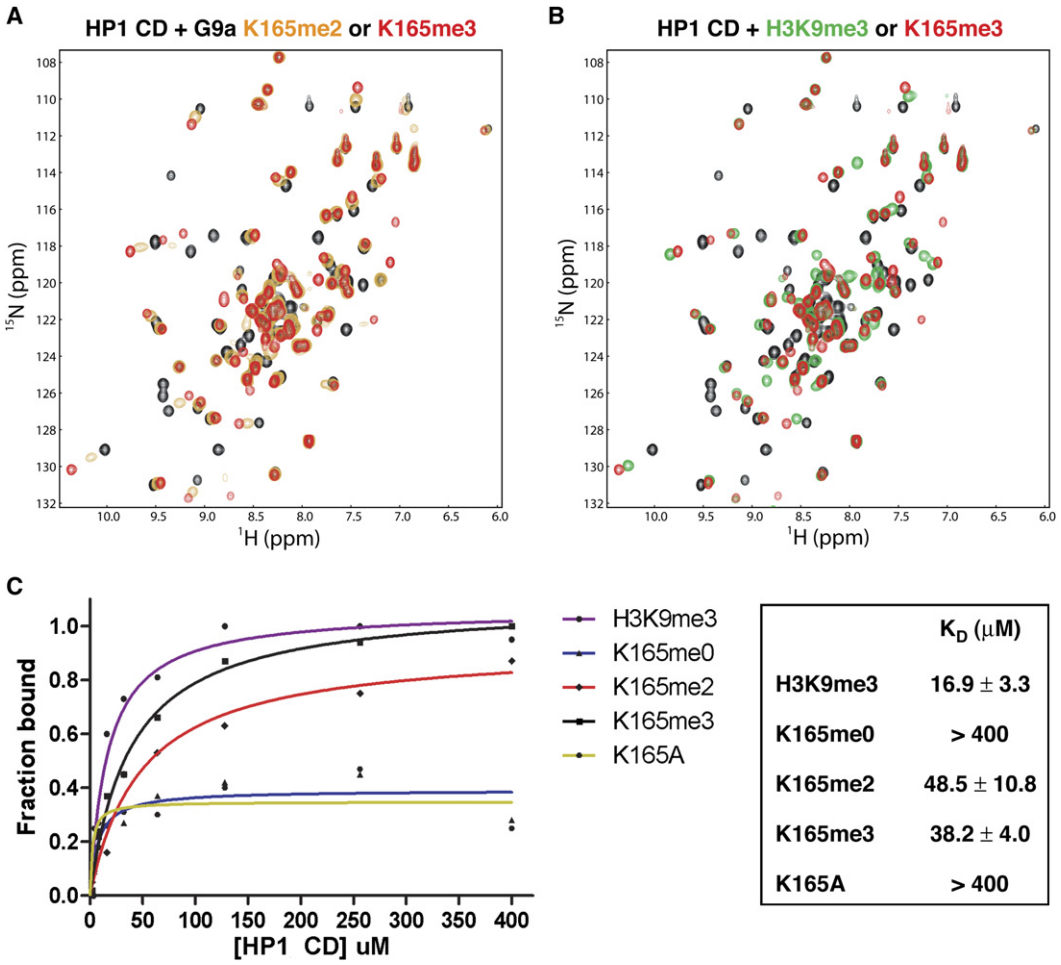


**Figure 5. Similar Binding Modes Underlie Chromodomain Recognition of G9a K165me and H3K9me**

(A) HSQC spectra overlay comparing HP1γ chromodomain in the absence (black) and presence of equimolar G9a K165me2 (orange) or G9a K165me3 (red) peptide. Peaks in the trimethylated spectrum undergo larger shifts from the unbound spectrum than do peaks in the dimethylated spectrum, indicating a higher-affinity interaction.

(B) HSQC spectra of HP1γ chromodomain in the presence of equimolar H3(1–20)K9me3 (green) or G9a K165me3 (red) peptide. In general, the same peaks undergo change in the presence of both peptides, implicating the same residues in both interactions.

(C) Fluorescence polarization analysis was performed using recombinant HP1γ chromodomain and the FITC-labeled peptides indicated. All assays were performed in triplicate, and the binding curve was fit to the data as described (Vinson et al., 1998). $K_D$ values (in micromolar) and the error of the fit for each peptide are shown to the right.

In order to directly measure these affinities, we next performed fluorescence polarization analysis of the HP1-H3K9me and HP1-K165me interactions using fluoresceinated peptides. As shown in Figure 5C, the $K_D$ for HP1-H3K9me3, -K165me3, and -K165me2 interaction were ~17, ~38, and ~48 μM, respectively, demonstrating that chromodomain-mediated recognition of H3K9 and G9a K165 occur within a comparable range of affinity. HP1γ chromodomain failed to bind either unmethylated K165 peptide (K165me0) or K165A mutant peptide, demonstrating that this interaction is both K165 and methylation dependent (Figure 5C). We conclude that the HP1γ chromodomain specifically recognizes methylated G9a through a binding mode similar to that of methyl-H3K9 recognition, and with comparable affinity.

## HP1 Interaction with Methyl-G9a Is Antagonized by Phosphorylation

The marked structural similarity between chromodomain-mediated recognition of methylated H3K9 and G9a K165 allowed modeling of the G9a-HP1 interaction onto the known X-ray crystal structure of the HP1 CD bound to H3K9me3 peptide (Jacobs and Khorasanizadeh, 2002). As is clear from this model (Figure 6A), both the size of the HP1 methyl-lysine binding cavity and the presence of an HP1γ acidic residue proximal to G9a T166 would disfavor nearby addition of a negatively charged phosphate group (Figure S8). The presence of a conserved phosphorylatable threonine (T166) adjacent to K165 led us to speculate that phosphorylation on this site could reverse G9a-HP1 interaction in a manner analogous to the

recently described H3K9-H3 serine 10 "methyl-phos switch" (Fischle et al., 2005; Hirota et al., 2005).

In the case of H3K9, mitotic H3S10 phosphorylation by the kinase Aurora B serves to release chromatin-bound HP1 (Fischle et al., 2005; Hirota et al., 2005). We therefore tested whether Aurora B could phosphorylate G9a T166. Indeed, both an H3(1–20) peptide and an unmodified G9a K165 peptide containing T166 were robustly phosphorylated in vitro by Aurora B complex (Figure 6B). This phosphorylation was not significantly affected by methylation on K165, consistent with recent reports demonstrating a minimal effect of H3K9 methylation on H3S10 phosphorylation by Aurora B in vitro (Fischle et al., 2005). We further found that a peptide synthesized to carry both K165 methylation and T166 phosphorylation was completely resistant to subsequent phosphorylation, demonstrating that the serine 10 kinase activity is specific for T166, the single residue aligning with H3 serine 10 (Figure 2B).

To determine whether phosphorylation of T166 can modulate G9a-HP1 interaction in vitro, immobilized unmodified, methylated, or methyl-phosphorylated G9a K165 peptides were incubated with in vitro-translated HP1$\gamma$ (Figure 6C, left; quantified at right). As expected, methylated K165 peptide bound HP1$\gamma$ strongly; however, this methyl-dependent binding was completely eliminated by concomitant phosphorylation on T166. The lack of HP1$\gamma$ binding to the methyl-phosphorylated G9a peptide was not due to reduced coupling efficiency of this peptide, since binding could be quantitatively restored by pretreatment of the phosphorylated peptide matrix with protein phosphatase 1 (Figure 6C). Consistent with this finding, a phospho-mimic threonine to glutamic acid substitution at position 166 (T166E) blocked interaction of G9a with HP1$\gamma$ in vivo (Figure 6D).

The antagonistic effect of T166 phosphorylation on HP1$\gamma$ CD binding to methylated G9a K165 could also be demonstrated by NMR, as titration of the HP1$\gamma$ CD with methyl-phosphorylated G9a K165 peptide induced a considerably smaller number of NMR perturbations when compared to titrations with methylated G9a K165 peptide (Figures 5B and 6E). Furthermore, the chemical shift changes observed with the methyl-phosphorylated peptide did not saturate at the maximal concentration tested, indicating that phosphorylation significantly weakens the interaction of G9a with the HP1 chromodomain.

### G9a Activity, but Not K165 Methylation, Is Required for Control of Gene Expression

Considering the known function of G9a as a transcriptional regulator (Shi et al., 2003; Tachibana et al., 2002), we tested the possibility that G9a methylation contributes to target gene regulation in vivo. Indirect immunofluorescence analysis of G9a$^{\Delta}$ cells demonstrated that complete G9a deficiency dramatically reduced euchromatic H3K9 dimethylation, with concomitant redistribution of HP1$\gamma$ from euchromatin to pericentric heterochromatin (Figure S9; Tachibana et al., 2002, 2005). These changes were associated with dysregulated expression of ~300–400 genes, as determined by comparing microarray gene expression analyses of G9a$^{\Delta}$ and G9a$^{WT}$ cells (Figure S10).

Similar changes were also seen in cells reconstituted with the G9a H1093K catalytic mutant, demonstrating that G9a methyltransferase activity is necessary for H3K9 dimethylation, HP1$\gamma$ localization, and proper in vivo control of gene expression (Figure 3B, Figures S9 and S10). In contrast, expression of the G9a K165A mutant caused only a mild increase in the amount of HP1$\gamma$ localized to pericentric heterochromatin (Figure S9), consistent with the unaltered levels and distribution of H3K9me2 in these cells (Figure 3B). Lack of K165 methylation likewise caused statistically significant dysregulation of only one gene, Hey1 (Figure S10).

## DISCUSSION

Starting from a sequence comparison, we have demonstrated that the histone methyltransferase G9a contains a lysine methylation cassette that mimics multiple features of histone lysine methylation, including sequence context, effector protein recognition, and secondary regulation by phosphorylation. Although striking on its own, there are indications that such histone-like modification cassettes—or histone mimics—may exist in many nonhistone proteins, particularly those that are chromatin associated, and may involve additional layers of complexity.

### Nonhistone Targets of Lysine Methylation

To date, attempts to identify targets of nonhistone lysine methylation have largely relied on candidate approaches, utilizing methyltransferases and/or putative targets of empiric interest (Chuikov et al., 2004; Kouskouti et al., 2004; Zhang et al., 2005). While an attempt was also recently made to identify methylated proteins in a more unbiased fashion using antibody enrichment and MS, all of the new targets identified were in fact arginine methylated (Ong et al., 2004). In contrast, our findings suggest that bioinformatic prediction of methylation targets may in fact be possible, based on similarity to known lysine methylation sites in histones. Our own initial analysis has yielded a number of proteins bearing evolutionarily conserved motifs likely to be targets of lysine methylation; strikingly, many of these are found within chromatin-associated proteins (S.C.S. and A.T., unpublished data).

Among the proteins found in this study to contain a potential methylation target site was mAM, a factor that binds to and regulates the catalytic activity of the essential H3K9 methyltransferase ESET (Wang et al., 2003). The human homolog of mAM (hAM) is recognized by our $\alpha$K165 me2 antibody (Figure 1E), and inspection of the hAM/mAM coding sequence identified a single conserved motif identical to G9a K165 and highly similar to H3K9 (Figure S2A and Figure 6F). Similarly, it was recently reported that HP1 is itself a target of phosphorylation on serine 83, a residue that we believe exists within an H3K9-like

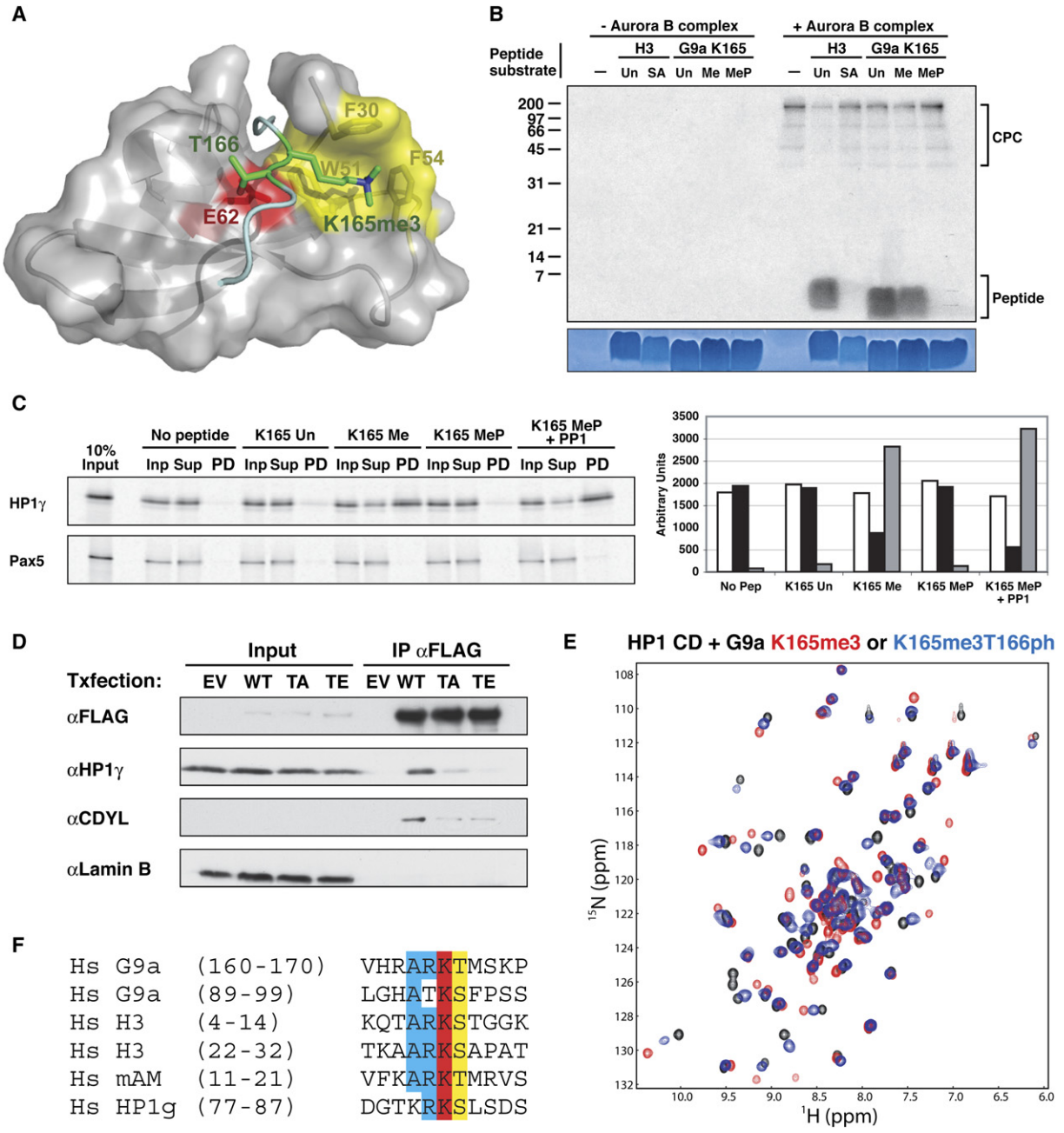


**Figure 6. Adjacent Phosphorylation Antagonizes Effector Protein Recognition of G9a K165 Methylation**

(A) Model of the HP1γ chromodomain (displayed as a ribbon beneath a transparent surface) bound to G9a K165me3 peptide. The side chains for G9a K165 and T166 are shown, as are the methyl-lysine binding "aromatic cage" residues of HP1γ (yellow surface) and an HP1γ acidic residue that could repel a phosphoryl group at T166 (E62; red surface).

(B) Phosphorylation of G9a T166 in vitro. G9a K165 peptides were phosphorylated in vitro using Aurora B-containing chromosomal passenger complex (CPC) immunoprecipitated from *Xenopus* egg extracts. An autoradiograph of the kinase assay is shown above and the Coomassie-stained peptide substrates below. The higher-molecular-weight species correspond to phosphorylation of known members of the CPC. Un, unmodified G9a K165 or H3 peptides; SA, H3 serine 10 to alanine mutant peptide; Me, G9a K165me2 peptide; MeP, G9a K165me2T166ph peptide.

(C) Phosphorylation of G9a T166 blocks HP1γ binding to K165. G9a K165 peptides covalently coupled to beads were incubated with in vitro-translated, $^{35}$S-radiolabeled HP1γ or Pax5 (control). After washing, the recovered protein was examined by SDS-PAGE and autoradiography (left, quantified on right). Beads were coupled with either buffer (No peptide), unmodified G9a K165 peptide (K165 Un), K165me2 peptide (K165 Me), K165me2T166ph peptide (K165 MeP), or K165me2T166ph peptide pretreated with protein phosphatase 1 (K165 MeP+PP1). Inp, input before addition of beads (open bars); Sup, supernatant after bead incubation (black bars); PD, pull-down fraction associated with beads (gray bars).

histone mimic (Lomberk et al., 2006, and Figure 6F). If so, this putative methylation site may in fact represent an intramolecular binding partner for the HP1 chromodomain, similar to the intramolecular SH2-phosphotyrosine interaction found in Src-family kinases (Roskoski, 2004).

The unexpected recurrence of H3K9 mimics in proteins associated with H3K9 methyltransferases (or, in the case of G9a and GLP, the methyltransferases themselves) suggests a complex interplay between histone and nonhistone methylation systems. While the functional details of this interplay are yet to be determined (see below), our recent observation that the H3K27 histone methyltransferase Ezh2 also undergoes automethylation (I. Su, M. Dobenecker, and A.T., unpublished data) suggests that self-methylation of HMTases and their associated proteins is likely to be a ubiquitous mode of HMTase regulation, analogous to kinase autophosphorylation. Furthermore, the emerging literature on effector modules for other histone methylation sites, such as H3K4 (Pray-Grant et al., 2005; Sims et al., 2005; Wysocka et al., 2005; reviewed in Kouzarides, 2007), suggests that methylation-dependent crosstalk between HMTases, their histone target sites, and nonhistone "mimics" of these sites may well be the rule rather than the exception.

## The G9a Modification System

The organization of the G9a "tail"—multiple methylation sites with similar sequences located in close proximity—raises a clear analogy to the H3 amino-terminal tail, in which recognition of methylated H3K9 and H3K27 are mediated by related but distinct classes of chromodomain-containing effectors (HP1 and Polycomb, respectively; Fischle et al. [2003b]). Since G9a K94 methylation is dispensable for both HP1 and CDYL binding (Figure 2C and data not shown), it is likely that distinct effector proteins are involved in recognition of methylated G9a K94. As with H3K9/K27, characterization of these K94-specific binding proteins may clarify functional similarities and differences between K165 and K94.

With regard to K165, it is now clear that this residue constitutes a binding site for at least two chromodomain proteins, HP1 and CDYL (Figures 4C and 4D). While K165-HP1 binding clearly requires K165 methylation (Figure 4A), it remains unclear which modification(s) mediates K165-CDYL interaction, as neither K165-unmodified, -methylated, or -methyl-phosphorylated peptides are capable of mediating G9a-CDYL interaction in vitro (data not shown). Adding further complexity to this situation, we note the potential existence of even more K165-binding proteins. For instance, in addition to G9a, GLP, and CDYL, previous purification of the CtBP repressor complex recovered Pc2, a chromodomain-containing SUMO E3 ligase (Shi et al., 2003). Although in vivo histone targets for the Pc2 CD are not known, it has been shown to bind in vitro to H3K9me3 peptides (Bernstein et al., 2006), and we in fact also observe in vitro binding of the Pc2 CD to K165me3 peptide (Figure S12). It should be noted, however, that G9a and Pc2 are localized within largely nonoverlapping nuclear domains (Saurin et al., 1998; Tachibana et al., 2001), and it is therefore uncertain whether G9a-Pc2 interaction occurs endogenously.

In addition to the further identification of K94/K165 binding partners, a final important mechanistic issue concerns regulation of K165-directed G9a catalytic activity. G9a is known to contribute significantly to H3K9 mono- and dimethylation, but not to trimethylation (Peters et al., 2003; Rice et al., 2003). In contrast, we observe di- and trimethylation of K165 by MS, but not monomethylation (Figure 2A and Figure S4). While these results may reflect technical difficulties in identifying monomethylated K165 (e.g., low abundance or concomitant modification on another site), we favor the view that the methyltransferase activity of G9a is altered in vivo to favor di- and trimethylation. Such a scenario is quite likely, given that the related HMTase ESET is regulated in this way by binding of the accessory protein mAM (Wang et al., 2003), and the fact that mAM is itself recognized by our αK165 me2 antibody (Figure 1E and Figure S2). Alternatively, it may be that a dedicated G9a K165 trimethylase exists in vivo, as is known to be the case for trimethylation of H3K9 (Peters et al., 2003; Rice et al., 2003).

## Functions of G9a Methylation

Determining the precise functions of G9a methylation, and of histone-like modification cassettes in general, clearly represents a central challenge for the future. Despite the obvious similarities between self-methylation of G9a and self-phosphorylation of Src-family kinases, a process known to regulate catalytic activity (Roskoski, 2004), we found no evidence of a role for G9a K165 methylation in regulation of G9a enzymatic function (Figure S11). Immunofluorescence analysis of G9a-deleted cells expressing nonmethylatable G9a$^{K165A}$ similarly demonstrated that G9a-HP1γ interaction is largely dispensable for euchromatic localization of both proteins (Figure S9). However, interpretation of these experiments is complicated by

(D) 293T cells were transfected with plasmids encoding either empty vector (EV), wild-type FLAG-G9a (WT), FLAG-G9a T166A (TA), or "phosphomimic" FLAG-G9a T166E (TE). The expressed proteins were immunoprecipitated and examined by western blot as indicated. Note that the T166A mutation reduces HP1γ binding but that this is even further suppressed by the T166E mutation; the increased countereffect of the T166E mutation is specific for HP1γ and is not seen with CDYL.

(E) HSQC spectra of HP1γ chromodomain in the presence of equimolar G9a K165me3 peptide with (blue) or without (red) adjacent phosphorylation at T166. The smaller shift changes in the presence of phosphorylation demonstrate that this modification strongly counteracts methyl-G9a binding to HP1γ.

(F) Protein sequence alignment of the human G9a K165 and K94 methylation sites with H3K9, H3K27, the H3K9-like site of human mAM (see Figure S2), and the predicted methylation site in HP1γ (see the Discussion). Complete identity is highlighted in red, five of six identity in blue, and shared phosphoacceptor sites in yellow.

the multiple layers of redundancy operating on the G9a methylation system, including the existence of multiple methylation sites, multiple effector proteins, and duplication of the entire pattern of G9a histone mimics on GLP, a protein known to heterodimerize with G9a in vivo (Tachibana et al., 2005). It is therefore likely that definitive answers regarding the functions of G9a methylation will require both single and combinatorial genetic ablation of G9a and GLP methylation sites; such studies are currently underway.

Despite the functional redundancy within this methylation system, several models can be envisaged for the function of G9a methylation in vivo. Histone mimics such as G9a K165 may allow effector-mediated targeting of associated proteins to particular nucleosomal sites (as has been suggested to occur for the H3K9 methyltransferase Suv39H; Maison and Almouzni, 2004) or conversely may increase the efficiency of effector protein loading onto histones. Since G9a exists in protein complexes containing HMTase, HDAC, and lysine demethylase activities (Ogawa et al., 2002; Shi et al., 2003), these enzymes may also regulate G9a function by directly modifying histone mimic sites and thereby defining the array of G9a-interacting effector proteins. Such a scenario would represent an exact parallel of the combinatorial readout proposed to occur on histones (Strahl and Allis, 2000). Importantly, while mammalian histones are not amenable to genetic analysis due to the multicopy nature of the histone genes (Maxson et al., 1983), such analysis is possible in the case of histone mimics. Therefore, in addition to their intrinsic interest and unique functions, histone mimics such as G9a K165 may unexpectedly provide the best system in a higher eukaryote in which to test fundamental predictions of the histone code hypothesis.

## EXPERIMENTAL PROCEDURES

Please see the Supplemental Experimental Procedures for additional protocols and experimental details.

### Generation of *G9a*$^{fl/fl}$ Mice

To create the *G9a* targeting vector, a BAC fragment (from RPCI24-165L4; BL/6; CHORI, USA) containing the murine *G9a* locus was subcloned into pBlueScriptIIKS+, and an oligonucleotide containing the 5′ loxP site was inserted into the intron separating exons 22 and 23. A fragment from pZeroloxP-FRT-neo-FRT(−) containing the 3′ loxP site and an FRT-flanked *neo* gene was inserted in the intron separating exons 24 and 25, and the resulting plasmid was subcloned into pDTA-TK to produce the final targeting construct. E14.1 (129/Ola) ES cells were transfected, selected, and used to produce chimeric mice as described (Torres and Kuhn, 1997). Chimeras were crossed to C57/BL6, and germline transmission was assessed by coat color. Deletion of the FRT-flanked *neo* gene was carried out by crossing of mice carrying the G9a$^{Targ}$ allele in the germline to FLPe-transgenic mice (Rodriguez et al., 2000). Induced *G9a* deletion produces out-of-frame splicing of exon 22 to exon 25, causing nonsense-mediated decay of the mutant transcript (data not shown). *G9a*-targeted mice were maintained on a mixed C57/BL6-129 genetic background and were housed in the Rockefeller University Laboratory Animal Resource Center under specific pathogen-free (SPF) conditions. All procedures were approved by the Institutional Animal Care and Use Committee (IACUC).

### Peptide Pull-Down Assays

G9a peptides were coupled to SulfoLink beads (Pierce) as per manufacturer's protocol. Twenty-five microliters (bed volume) of beads were added to nuclear extracts (prepared as above), rotated overnight at 4°C, washed five times with M2 lysis buffer (50 mM Tris-HCl [pH 7.4], 150 mM NaCl, 1 mM EDTA, 1% Triton X-100), and boiled in 1 × Laemmli sample buffer. Binding to in vitro-translated proteins was performed essentially as described (Lachner et al., 2001). Where necessary, peptides were first dephosphorylated with 25 units PP1 (NEB) as per manufacturer's protocol. Samples were separated by 7.5%–15% linear gradient SDS-PAGE, stained with Coomassie blue, dried, and exposed to a PhosphorImager.

For Pc2 pull-down, peptides coupled as above were incubated with 5 μg recombinant Pc2 CD-GST fusion protein (kind gift of E. Bernstein and C.D. Allis) and a 20-fold excess of BSA in assay buffer (150 mM NaCl, 50 mM Tris-Cl [pH 8.0], 1% NP-40). Beads were washed six times in assay buffer followed by PAGE and staining with colloidal Coomassie blue.

### NMR Spectroscopy

Uniformly $^{15}$N-labeled HP1γ protein (pET16b, residues 20–70) was expressed by growing *E. coli* BL21(DE3) bacteria in minimal medium supplemented with $^{15}NH_4Cl$ as the sole nitrogen source and inducing with 1 mM IPTG for 16 hr at 18°C. The protein was purified using nickel-NTA affinity and size-exclusion chromatography. NMR samples contained 0.5 mM protein in PBS at pH 7.4, 5 mM DTT-$d_{10}$, and 10% $D_2O$. Peptides were dissolved in NMR buffer prior to addition to samples. All NMR spectra were acquired on Bruker 500 or 600 MHz spectrometers at 25°C. The model of HP1γ CD bound to G9a K165me3 peptide was calculated using MODELER based on previous structures of the HP1 chromodomain bound to methylated H3 peptides (PDB codes 1KNE and 1GUW).

### Mass Spectrometry Analysis

Purified FLAG-G9a protein expressed by transient transfection in 293T cells was digested with trypsin, and mass spectra were obtained using an in-house-modified MALDI-QqTOF mass spectrometer equipped with a compact disc (CD) sample stage (Krutchinsky et al., 2000, 2001). Masses of tryptic peptides were determined with 10 ppm accuracy. After obtaining tryptic maps of proteins in the QqTOF mass spectrometer, the CD MALDI target was transferred to an in-house-constructed MALDI ion trap mass spectrometer for detailed MS/MS analysis of the tryptic peptide ions (Krutchinsky et al., 2001).

### Fluorescence Polarization

Anisotropy binding assays (Vinson et al., 1998) were performed essentially as described (Fischle et al., 2003b). HP1γ chromodomain was expressed and purified as for NMR (see the Supplemental Experimental Procedures), and binding was analyzed in assay buffer (50 mM $Na_2HPO_4$ [pH 7.0], 25 mM NaCl, 1 mM $MgCl_2$, 2 mM DTT).

### Peptides

All G9a peptides were produced by the Rockefeller University Proteomics Resource Center and were at least 85% pure. All G9a peptides included an exogenous C-terminal cysteine; G9a K165 peptides contained hG9a residues 159–171 (final sequence, KVHRARKTMSKPGC), and G9a K94 peptides contained hG9a residues 88–100 (final sequence, LLGHATKSFPSSPC). H3 peptides were kindly provided by C.D. Allis (Rockefeller University).

### Antibodies

Sources and working dilutions of antibodies for western blotting were as follows: αG9a-N (RU1061), rabbit, 1 μg/ml; α4xH3K9me2 (kind gift of T. Jenuwein, IMP, Vienna), rabbit, 6 μg/ml; α-tubulin (DM-1A;

Sigma), mouse, 1:5000; α-FLAG M2 (Sigma), mouse, 10 μg/ml; αMeK165 (RU1218), rabbit, 2 μg/ml; α-lamin B (Santa Cruz Biotech), goat, 1:500; αHP1γ (Upstate), rabbit, 1:500; αHP1α (Upstate), rabbit, 1:500; and αdiMeH3K9 (Upstate, #07-212), rabbit, 1:500.

### Supplemental Data

Supplemental Data include Supplemental Experimental Procedures, 12 figures, and Supplemental References and can be found with this article online at http://www.molecule.org/cgi/content/full/27/4/596/DC1/.

## ACKNOWLEDGMENTS

We thank T. Jenuwein (IMP, Vienna) for the gifts of α4xH3K9 me2 antibody and HP1 expression constructs; E. Bernstein and C.D. Allis (Rockefeller University, NY) for recombinant Pc2 CD-GST protein and H3 peptides; D. O'Carroll for help with conditional mutagenesis; A. Kelly for help with NMR analysis; C. Karan and E. Bernstein for assistance with fluorescence polarization experiments; H. Zebroski for peptide synthesis; C. Schmedt and A. Kelly for critical reading of the manuscript; and C.D. Allis, C. Rice, C. Nathan, and P. Nurse for stimulating discussions. S.C.S. was supported by the Rudin Foundation and by National Institutes of Health Medical Scientist Training Program grant GM07739 to the Cornell/Rockefeller/Sloan-Kettering Tri-Institutional MD-PhD program. K.L.Y. was supported by a fellowship from the Terry Fox Foundation through the National Cancer Institute of Canada. Work in the lab of A.T. is supported by the Irene Diamond Foundation. B.T.C. acknowledges National Institutes of Health NCRR Grant R00862 for support.

Received: February 12, 2007
Revised: May 19, 2007
Accepted: June 12, 2007
Published: August 16, 2007

## REFERENCES

Bannister, A.J., Zegerman, P., Partridge, J.F., Miska, E.A., Thomas, J.O., Allshire, R.C., and Kouzarides, T. (2001). Selective recognition of methylated lysine 9 on histone H3 by the HP1 chromo domain. Nature *410*, 120–124.

Bernstein, E., Duncan, E.M., Masui, O., Gil, J., Heard, E., and Allis, C.D. (2006). Mouse polycomb proteins bind differentially to methylated histone H3 and RNA and are enriched in facultative heterochromatin. Mol. Cell. Biol. *26*, 2560–2569.

Byvoet, P., Shepherd, G.R., Hardin, J.M., and Noland, B.J. (1972). The distribution and turnover of labeled methyl groups in histone fractions of cultured mammalian cells. Arch. Biochem. Biophys. *148*, 558–567.

Caron, C., Pivot-Pajot, C., van Grunsven, L.A., Col, E., Lestrat, C., Rousseaux, S., and Khochbin, S. (2003). Cdyl: a new transcriptional co-repressor. EMBO Rep. *4*, 877–882.

Chuikov, S., Kurash, J.K., Wilson, J.R., Xiao, B., Justin, N., Ivanov, G.S., McKinney, K., Tempst, P., Prives, C., Gamblin, S.J., et al. (2004). Regulation of p53 activity through lysine methylation. Nature *432*, 353–360.

Dillon, S.C., Zhang, X., Trievel, R.C., and Cheng, X. (2005). The SET-domain protein superfamily: protein lysine methyltransferases. Genome Biol. *6*, 227. Published online August 2, 2005. 10.1186/gb-2005-6-8-227.

Fischle, W., Wang, Y., and Allis, C.D. (2003a). Binary switches and modification cassettes in histone biology and beyond. Nature *425*, 475–479.

Fischle, W., Wang, Y., Jacobs, S.A., Kim, Y., Allis, C.D., and Khorasanizadeh, S. (2003b). Molecular basis for the discrimination of repressive methyl-lysine marks in histone H3 by Polycomb and HP1 chromodomains. Genes Dev. *17*, 1870–1881.

Fischle, W., Tseng, B.S., Dormann, H.L., Ueberheide, B.M., Garcia, B.A., Shabanowitz, J., Hunt, D.F., Funabiki, H., and Allis, C.D. (2005). Regulation of HP1-chromatin binding by histone H3 methylation and phosphorylation. Nature *438*, 1116–1122.

Hirota, T., Lipp, J.J., Toh, B.H., and Peters, J.M. (2005). Histone H3 serine 10 phosphorylation by Aurora B causes HP1 dissociation from heterochromatin. Nature *438*, 1176–1180.

Huang, J., Perez-Burgos, L., Placek, B.J., Sengupta, R., Richter, M., Dorsey, J.A., Kubicek, S., Opravil, S., Jenuwein, T., and Berger, S.L. (2006). Repression of p53 activity by Smyd2-mediated methylation. Nature *444*, 629–632.

Jacobs, S.A., and Khorasanizadeh, S. (2002). Structure of HP1 chromodomain bound to a lysine 9-methylated histone H3 tail. Science *295*, 2080–2083.

Kouskouti, A., Scheer, E., Staub, A., Tora, L., and Talianidis, I. (2004). Gene-specific modulation of TAF10 function by SET9-mediated methylation. Mol. Cell *14*, 175–182.

Kouzarides, T. (2007). Chromatin modifications and their function. Cell *128*, 693–705.

Krutchinsky, A.N., Zhang, W., and Chait, B.T. (2000). Rapidly switchable matrix-assisted laser desorption/ionization and electrospray quadrupole-time-of-flight mass spectrometry for protein identification. J. Am. Soc. Mass Spectrom. *11*, 493–504.

Krutchinsky, A.N., Kalkum, M., and Chait, B.T. (2001). Automatic identification of proteins with a MALDI-quadrupole ion trap mass spectrometer. Anal. Chem. *73*, 5066–5077.

Lachner, M., O'Carroll, D., Rea, S., Mechtler, K., and Jenuwein, T. (2001). Methylation of histone H3 lysine 9 creates a binding site for HP1 proteins. Nature *410*, 116–120.

Lahn, B.T., Tang, Z.L., Zhou, J., Barndt, R.J., Parvinen, M., Allis, C.D., and Page, D.C. (2002). Previously uncharacterized histone acetyltransferases implicated in mammalian spermatogenesis. Proc. Natl. Acad. Sci. USA *99*, 8707–8712.

Lindroth, A.M., Shultis, D., Jasencakova, Z., Fuchs, J., Johnson, L., Schubert, D., Patnaik, D., Pradhan, S., Goodrich, J., Schubert, I., et al. (2004). Dual histone H3 methylation marks at lysines 9 and 27 required for interaction with CHROMOMETHYLASE3. EMBO J. *23*, 4286–4296.

Lomberk, G., Bensi, D., Fernandez-Zapico, M.E., and Urrutia, R. (2006). Evidence for the existence of an HP1-mediated subcode within the histone code. Nat. Cell Biol. *8*, 407–415.

Maison, C., and Almouzni, G. (2004). HP1 and the dynamics of heterochromatin maintenance. Nat. Rev. Mol. Cell Biol. *5*, 296–304.

Margueron, R., Trojer, P., and Reinberg, D. (2005). The key to development: interpreting the histone code? Curr. Opin. Genet. Dev. *15*, 163–176.

Maxson, R., Cohn, R., Kedes, L., and Mohun, T. (1983). Expression and organization of histone genes. Annu. Rev. Genet. *17*, 239–277.

Ogawa, H., Ishiguro, K., Gaubatz, S., Livingston, D.M., and Nakatani, Y. (2002). A complex with chromatin modifiers that occupies E2F- and Myc-responsive genes in G0 cells. Science *296*, 1132–1136.

Ong, S.E., Mittler, G., and Mann, M. (2004). Identifying and quantifying in vivo methylation sites by heavy methyl SILAC. Nat. Methods *1*, 119–126.

Paik, W.K., and Kim, S. (1971). Protein methylation. Science *174*, 114–119.

Perez-Burgos, L., Peters, A.H., Opravil, S., Kauer, M., Mechtler, K., and Jenuwein, T. (2004). Generation and characterization of methyl-lysine histone antibodies. Methods Enzymol. *376*, 234–254.

Peters, A.H., Kubicek, S., Mechtler, K., O'Sullivan, R.J., Derijck, A.A., Perez-Burgos, L., Kohlmaier, A., Opravil, S., Tachibana, M., Shinkai, Y., et al. (2003). Partitioning and plasticity of repressive histone methylation states in mammalian chromatin. Mol. Cell *12*, 1577–1589.

Pray-Grant, M.G., Daniel, J.A., Schieltz, D., Yates, J.R., III, and Grant, P.A. (2005). Chd1 chromodomain links histone H3 methylation with SAGA- and SLIK-dependent acetylation. Nature *433*, 434–438.

Rea, S., Eisenhaber, F., O'Carroll, D., Strahl, B.D., Sun, Z.W., Schmid, M., Opravil, S., Mechtler, K., Ponting, C.P., Allis, C.D., and Jenuwein, T. (2000). Regulation of chromatin structure by site-specific histone H3 methyltransferases. Nature *406*, 593–599.

Rice, J.C., Briggs, S.D., Ueberheide, B., Barber, C.M., Shabanowitz, J., Hunt, D.F., Shinkai, Y., and Allis, C.D. (2003). Histone methyltransferases direct different degrees of methylation to define distinct chromatin domains. Mol. Cell *12*, 1591–1598.

Rodriguez, C.I., Buchholz, F., Galloway, J., Sequerra, R., Kasper, J., Ayala, R., Stewart, A.F., and Dymecki, S.M. (2000). High-efficiency deleter mice show that FLPe is an alternative to Cre-loxP. Nat. Genet. *25*, 139–140.

Roopra, A., Qazi, R., Schoenike, B., Daley, T.J., and Morrison, J.F. (2004). Localized domains of G9a-mediated histone methylation are required for silencing of neuronal genes. Mol. Cell *14*, 727–738.

Roskoski, R., Jr. (2004). Src protein-tyrosine kinase structure and regulation. Biochem. Biophys. Res. Commun. *324*, 1155–1164.

Sarma, K., Nishioka, K., and Reinberg, D. (2004). Tips in analyzing antibodies directed against specific histone tail modifications. Methods Enzymol. *376*, 255–269.

Saurin, A.J., Shiels, C., Williamson, J., Satijn, D.P., Otte, A.P., Sheer, D., and Freemont, P.S. (1998). The human polycomb group complex associates with pericentromeric heterochromatin to form a novel nuclear domain. J. Cell Biol. *142*, 887–898.

Shi, Y., Sawada, J., Sui, G., Affar el, B., Whetstine, J.R., Lan, F., Ogawa, H., Luke, M.P., and Nakatani, Y. (2003). Coordinated histone modifications mediated by a CtBP co-repressor complex. Nature *422*, 735–738.

Sims, R.J., III, Chen, C.F., Santos-Rosa, H., Kouzarides, T., Patel, S.S., and Reinberg, D. (2005). Human but not yeast CHD1 binds directly and selectively to histone H3 methylated at lysine 4 via its tandem chromodomains. J. Biol. Chem. *280*, 41789–41792.

Strahl, B.D., and Allis, C.D. (2000). The language of covalent histone modifications. Nature *403*, 41–45.

Tachibana, M., Sugimoto, K., Fukushima, T., and Shinkai, Y. (2001). Set domain-containing protein, G9a, is a novel lysine-preferring mammalian histone methyltransferase with hyperactivity and specific selectivity to lysines 9 and 27 of histone H3. J. Biol. Chem. *276*, 25309–25317.

Tachibana, M., Sugimoto, K., Nozaki, M., Ueda, J., Ohta, T., Ohki, M., Fukuda, M., Takeda, N., Niida, H., Kato, H., and Shinkai, Y. (2002). G9a histone methyltransferase plays a dominant role in euchromatic histone H3 lysine 9 methylation and is essential for early embryogenesis. Genes Dev. *16*, 1779–1791.

Tachibana, M., Ueda, J., Fukuda, M., Takeda, N., Ohta, T., Iwanari, H., Sakihama, T., Kodama, T., Hamakubo, T., and Shinkai, Y. (2005). Histone methyltransferases G9a and GLP form heteromeric complexes and are both crucial for methylation of euchromatin at H3-K9. Genes Dev. *19*, 815–826.

Torres, R.M., and Kuhn, R. (1997). Laboratory Protocols for Conditional Gene Targeting (Oxford: Oxford University Press).

Vinson, V.K., De La Cruz, E.M., Higgs, H.N., and Pollard, T.D. (1998). Interactions of Acanthamoeba profilin with actin and nucleotides bound to actin. Biochemistry *37*, 10871–10880.

Wang, H., An, W., Cao, R., Xia, L., Erdjument-Bromage, H., Chatton, B., Tempst, P., Roeder, R.G., and Zhang, Y. (2003). mAM facilitates conversion by ESET of dimethyl to trimethyl lysine 9 of histone H3 to cause transcriptional repression. Mol. Cell *12*, 475–487.

Wysocka, J., Swigut, T., Milne, T.A., Dou, Y., Zhang, X., Burlingame, A.L., Roeder, R.G., Brivanlou, A.H., and Allis, C.D. (2005). WDR5 associates with histone H3 methylated at K4 and is essential for H3 K4 methylation and vertebrate development. Cell *121*, 859–872.

Zhang, K., Yau, P.M., Chandrasekhar, B., New, R., Kondrat, R., Imai, B.S., and Bradbury, M.E. (2004). Differentiation between peptides containing acetylated or tri-methylated lysines by mass spectrometry: an application for determining lysine 9 acetylation and methylation of histone H3. Proteomics *4*, 1–10.

Zhang, K., Lin, W., Latham, J.A., Riefler, G.M., Schumacher, J.M., Chan, C., Tatchell, K., Hawke, D.H., Kobayashi, R., and Dent, S.Y. (2005). The Set1 methyltransferase opposes Ipl1 aurora kinase functions in chromosome segregation. Cell *122*, 723–734.